*Geologie en Mijnbouw* **73:** 365–374, 1994.



# Liquefaction potential and dewatering injection structures at Herkenbosch: field investigations of the effects of the 1992 Roermond earthquake, the Netherlands

C.A. Davenport[1], J.M.J. Lap[2], P.M. Maurenbrecher[3] & D.G. Price[3]
[1] *University of East Anglia, School of Environmental Sciences, Norwich NR4 7TJ, UK;* [2] *formerly Delft University of Technology;* [3] *Engineering Geology Section, Delft University of Technology, the Netherlands*

Received 10 June 1993; accepted in revised form 15 April 1994

*Key words:* earthquake-induced liquefaction, sand fissures and mounds, excavations

## Abstract

Near-surface soils in the southern Netherlands include fine sands with, in some areas, a watertable at shallow depth. A reconnaissance study undertaken in 1987 to ascertain the potential for a liquefaction hazard in areas south of Eindhoven revealed a high liquefaction potential in the area around and to the south of Roermond. The earthquake of 13 April 1992 caused sand eruptions to occur in numerous locations in the vicinity of Roermond. This study focuses on sand fissures and mounds located to the south of Herkenbosch, between the town and the River Roer. Excavations revealed extensive disturbance of clay and silt deposits down to confined saturated sand deposits at depths of several metres below the surface. Extensive ground cracking, with or without sand extrusion, occurred over an area of circa 0.5 km$^2$. Pit and trench excavations permitted detailed mapping and sampling of over 30 m of sand-injected fissures. The evidence indicates that ground cracks were injected, almost passively, by sand entrained within water, driven upwards following liquefaction of the previously confined sand. Groundwater conditions are such that sand volcanoes and spring pits developed at the bottom of the deeper excavations.

## Introduction

On 13 April 1992 at 3.20 am local time, an earthquake of magnitude $M_L = 5.9 \pm 0.1$ rocked a large area of the southern Netherlands and adjacent areas of Germany and Belgium (Ahorner 1993). In the epicentral area walls and roofs collapsed and church towers cracked. Witnesses report ground waves, ground cracking, and sand fountains in the area south of Herkenbosch, near to industrial complexes. The only reported earthquake-induced landslides in the Netherlands occurred at Brunssum. In the city of Roermond many historic buildings were seriously damaged, including the famous Munster church, ornate roofs near the railway station, and brickwork of the Vroom & Dreesmann department store. River bank collapses, ground cracking and damage to building foundations were also documented.

During May through November 1992 the authors, assisted by students of the Engineering Geology Section of the Faculty of Mining and Petroleum Engineering of Delft University of Technology, investigated geotechnical phenomena at Herkenbosch and Brunssum (Maurenbrecher et al. 1994). This paper reports findings of the initial evaluation of the results of the liquefaction of a confined sand layer in the floodplain of the River Roer south of Herkenbosch (Fig. 1). Earlier studies of liquefaction potential by Lap in 1987 are also reported (Lap 1987).

## Liquefaction potential study

Liquefaction potential was evaluated for the Netherlands south of latitude 51° 30′ and east of longitude 5°, an area which includes large parts of the provinces of Limburg and Noord Brabant. A simplified procedure was used to obtain a first-order scenario based upon the geological, hydrogeological and geotechnical data available to Lap during the period 1986–

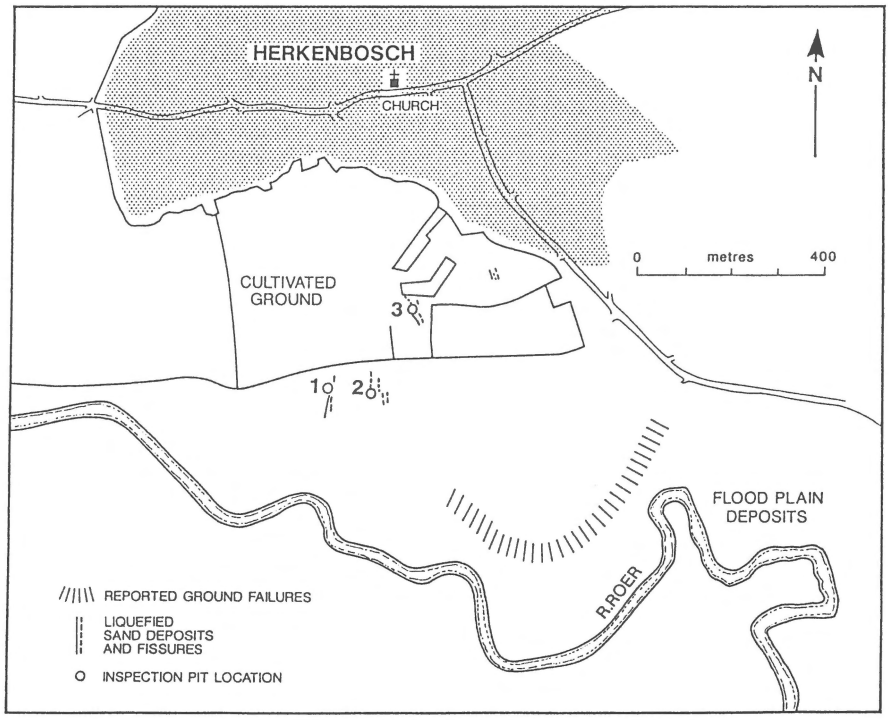


*Fig. 1.* Location of liquefaction deposits and trenches (sites 1–3), south of Herkenbosch, April 1992.

87 (Lap 1987). In 1987 the study was extended to identify areas where earthquake-induced liquefaction was most likely to have taken place in the historical and pre-historical domains. Of particular interest is the possibility that pre-historical (palaeoseismic) ground deformation could provide a basis for improving the database for long-term hazard assessment in the Netherlands. The study comprised two parts: (i) the identification of susceptible deposits, and (ii) the quantification of liquefaction opportunity using simplified classical methods (Seed & Idriss 1971, Tinsley et al. 1985). The effects of the 1992 event provided a unique opportunity to test the value of this approach.

*Liquefaction susceptibility*

The geological and hydrogeological factors and data sources influencing susceptibility classification are:

– age and type of sediment – from geological maps,

– looseness of sand – from geotechnical data,

– depth of groundwater – from hydrogeological maps and boreholes.

The results of the engineering geological assessment of the deposits are summarised in Table 1. Of the older Quaternary deposits, only the Kedichem 'porridge' sands and the Twente sands have susceptibility. In South Limburg, only the Twente Formation has appropriate soil types. The Holocene deposits are generally more susceptible; however, loess and organic-rich deposits are not included. Mine tailings, river embankments and dykes may well be vulnerable, but were not considered in this study.

The identification of saturated zones was based upon published groundwater maps (Dienst Grondwater Verkenning 1974). Where possible, groundwater contour maps were prepared and overlaid on topography for areas where susceptible soil types could be identified. In general, groundwater levels are close to the

*Table 1.* Liquefaction susceptibility of geological units south of Eindhoven

| Formation name | Synoptic description | Maximum thickness (m) | Susceptibility (S) n = not: p = partial |
|---|---|---|---|
| HOLOCENE | | | |
| Griendtsveen | peat | 4 | Sn |
| Singraven | fluvial | 1 | Sp |
| Kootwijk | eolian sand | 4 | S |
| Betuwe | sands and clays | 1 | Sp |
| PLEISTOCENE | | | |
| Twente | cover sands (top), loess, peat | 25 | S |
| Kreftenheye | fluvial, coarse | ? | Sn |
| Asten | peat, with clay | ? | Sn |
| Eindhoven | complex of sand, loess, peat and gravel | 25 | Sn |
| Veghel | fluvial, coarse | 20 | Sn |
| Sterksel | fluvial, coarse | 60 | Sn |
| Kedichem | fluvial, fine to coarse sands | 10 | S |
| Tegelen | fluvial, coarse, sand and clays | 100 | Sn |

surface (down to 2 m). Seasonal variations were not included. In the calculations of liquefaction potential in the area around Roermond, water depths were taken directly from field test data.

Maps were prepared for each formation. The distribution of susceptible deposits formed the basis of a liquefaction potential map.

*Liquefaction potential*

The region was divided into a number of areas for liquefaction opportunity assessment. The simplified procedure of Seed & Idriss (1971) was followed. The basic principle involves comparison of the shear stresses induced by the earthquake with the stresses required to cause liquefaction in situ. The key decisions required are as follows:

*Number of stress cycles* – an earthquake-magnitude estimate is required. Moreover, the location of the event with respect to the deposit needs to be considered.

*Peak ground acceleration* – for distances greater than 25 km, the attenuation relationship of Donovan (1973) was used. For closer distances, the results obtained by Joyner & Fumal (1985) are applied. Intensity–acceleration relationships applied to published expected intensity maps were used to provide additional ground motion estimates and convert other estimates to intensity (Trifunac & Brady 1975, Nason 1982, Evernden & Thomson 1985). Assuming that a 'locked up' segment on the Peel Boundary Fault south of Roermond explains the 'gap' in seismicity between Uden (1932) and Düren (1755, 1756), the location of a future (large) event was taken to be on the Peel Boundary Fault near to Roermond.

*Geotechnical properties* – the Twente formation data provides a $D_{50}$ (grainsize diameter at 50% retention) range of 0.125 mm to 0.25 mm with a mean of 0.19. Cone Penetration Test (CPT) values provided by Soil Mechanics, Delft, yielded geological depth profiles. South of Roermond, the Twente Formation has a water level depth of 2 m, a critical depth of ca. 6 m, and a CPT range of 2–8 MPa.

The factor of safety (F) against liquefaction (Seed & Idriss 1971) is given by:

$$F = \frac{\tau}{\tau_{av}}$$

for relative density (Dr) values of 15% and 50% for a range of earthquake intensities (Table 2, where $\tau$ and $\tau_{av}$ are defined). A liquefaction field can be plotted, as shown in Fig. 2.

Lap (1987) concluded that 'the fluvio-glacial deposits in areas south of Roermond have a high liquefaction potential. At the maximum expected intensity value of VII, liquefaction will be generated. The porridge sands east of Venlo are even more likely to liquefy'.

*Table 2.* Liquefaction potential analysis for the area south of Roermond using Seed & Idriss (1971).

Assumptions

M = 6 earthquake on the Peel Boundary Fault. 8 Cycles of strong ground motion shaking, depth of 6 m below ground level (b.g.l.).
Loose – medium dense sands Twente Formation (late Quaternary)
Water table at 2 m b.g.l

Stresses required to cause liquefaction

In-situ geotechnical properties:
Dr range 15–50%; Cr range 0.54–0.57
Normal effective stress ($\sigma_0$) of 71.5 $kNm^{-2}$ at 6 m b.g.l.,
CPT range 2–8 MPa
$D_{50}$ range 0.125–0.25 mm : average 0.19 mm
Stress ratio ($\alpha$) = 0.246

$$\tau = \alpha * \sigma_0 * Dr_{50} * Cr$$

Dr = 15% : $Dr_{50}$ = 0.3 : $\tau$ = 2.85 $kNm^{-2}$
Dr = 50% : $Dr_{50}$ = 1.0 : $\tau$ = 9.82 $kNm^{-2}$

Stresses induced by M = 6 earthquake

Stress scaling factor ($\times \tau_{max}$) = 0.65
Average unit weight ($\sigma$) = 20 $kNm^{-3}$
Depth of initial liquefaction data from California = $a_{max}$ (g)
Stress reduction factor (for depth) (rd) = 0.96

$$\tau_{av} = 0.65 * (\sigma_h * (a_{max}(g)) * rd$$

| Intensity (MM) | $a_{max}$(g) | $\tau_{av}$ ($kNm_{-2}$) |
|---|---|---|
| V - VI | 0.05 | 3.7 |
| VI | 0.08 | 6.0 |
| VI - VII | 0.11 | 8.2 |
| VII | 0.15 | 11.2 |
| VII - VIII | 0.19 | 14.2 |
| VIII | 0.25 | 18.7 |
| VIII - IX | 0.33 | 24.7 |
| IX | 0.42 | 31.4 |

Factor of safety (F) (against liquefaction) $F = \frac{\tau}{\tau_{av}}$

| Dr = 15% | | Dr = 50% | |
|---|---|---|---|
| Intensity (MM) | F | Intensity (MM) | F |
| V - VI | 0.77 | V - VI | 2.65 |
| VI | 0.48 | VI | 1.64 |
| VI - VII | 0.35 | VI - VII | 1.20 |
| VII | 0.26 | VII | 0.88 |
| VII - VIII | 0.20 | VII - VIII | 0.69 |

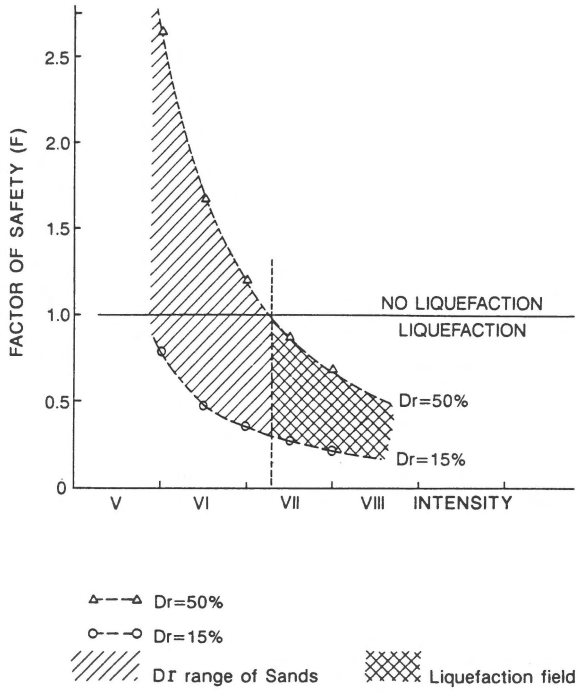


*Fig. 2.* Graph showing liquefaction field in Intensity versus factor of safety diagram for the Twente Formation at 6 m depth.

The liquefaction potential map is given in Fig. 3, using the following criteria:

| | | | | | |
|---|---|---|---|---|---|
| 0 | < | F | < | 0.5 | high |
| 0.5 | < | F | < | 0.75 | medium |
| 0.75 | < | F | < | 1.0 | low |

In fact, all areas with $F < 1.0$ have a liquefaction hazard potential, particularly near faults. Lap concluded that 'the results obtained can serve as a satisfactory indication of what will happen in the area under consideration during earthquakes'.

## Liquefaction at Herkenbosch

In the early hours of 13 April 1992 the small towns south of Roermond and west of the Peel Boundary Fault were shaken strongly. Vulnerable building structures and foundations were damaged, particularly close to the river Roer. Maximum intensities (MSK) of up to VII + are attributable to small areas of low ground lying on the downthrown side of the Peel Boundary Fault. Herkenbosch is located in such an area. Here the vulnerability of the ground to earthquake-induced damage can be demonstrated clearly. On the cultivated dark clayey soils south of the town, early-morning witnesses report jelly-like soft patches of ground and (temporary) surface water. Long lines of pale-coloured sand formed glistening ridges, interrupted by larger mounds up to 200 mm in height. Within days, the mounds and ridges had slumped into low-relief sand patches. Detailed inspection of the larger elongated patches (lying closer to the river) revealed linear depressions suggesting the presence of near-continuous fissures beneath each sand patch. By the time the sand patches has been located and mapped, the sugar beet crop had risen. Detailed survey and excavation of the fissures had to wait until November. A small bucket excavator, also used for archaeological excavations, was used to excavate three trench systems, shown as Pits 1, 2 and 3 on Fig. 1. Initially, shallow trenches to depths of up to 0.5 m were constructed normal to and along the line of the sand patches in order to locate the feeder fissures. Incremential deepening allowed the 3-D structure of damage to be mapped. Locally, these trenches were deepened to ascertain the depth to the underlying sand; the greatest depth being 2.85 m below ground level (b.g.l.) in Pit 2. In each case, a superficial layer of brown clayey silt and silty clay (silt-clay) was excavated which was virtually structureless and generally over 2 m in thickness. Excavations were dry except when the underlying sand was reached, the sand being saturated by groundwater under a small piezometric pressure. Consequently, water and sand 'boiled' up in the bottom of Pit 3 to a depth of 100 mm, giving a water level corresponding to those measured in earlier boreholes (i.e. 2 m b.g.l.). In the floor of Pit 3, water seeped under pressure out of a sand-filled fissure and eventually small sand mounds emerged above the rising water.

The pits stayed open for several hours, showing few signs of instability on vertical faces without support. However, cracking of the ground was encountered below the line of the surface patches and even beyond the areas of surface expression. Some cracks were sand-filled, others not; some reached the surface, and others not. Many secondary fine (usually sand-filled) fissures can be traced away from the main suite, not only branching but occasionally anastomosing. The main suite of fissures has been mapped in detail at various depths. Shallow depths, such as 0.3 m and 0.5 m b.g.l., provided the clearest contrasts between sand-filled fissures and the darkly weathered silt-clay (Fig. 4). For the greatest part, the fissures are up to 10 mm wide, locally becoming wider and occasionally

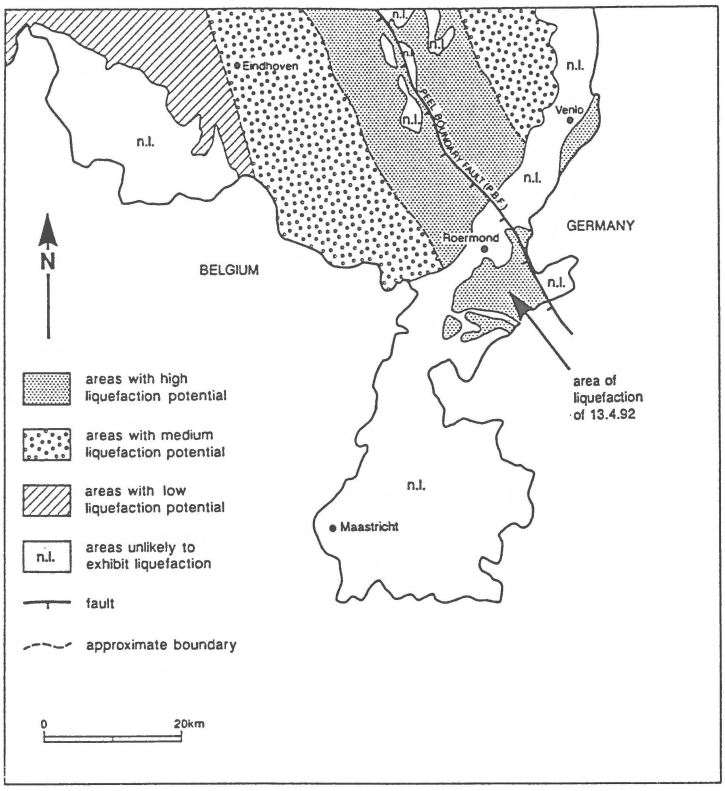


*Fig. 3.* Map of liquefaction for a future magnitude 6 earthquake along the Peel Boundary Fault (after Lap 1987).

interrupted by pipes. (Some pipes may be infilled root or worm-holes.) The main suite forms a macroscale pattern in plan which resembles left-lateral shear segments (en echelon). Remarkably, smaller-scale segments (usually less than 0.5 m in length) are arranged also in a left-lateral en echelon array. Evidence of oblique movement has not been detected either on fissure surfaces or in the intervening 'pseudotranstension' zones. Overall, the length mapped was over 30 m in total, with no signs that fissuring ceases, at least at depth.

A composite block diagram has been produced from the range of features to illustrate their relationships and relative dimensions (Fig. 5). In the floors of Pits 2 and 3, the fissures widen as they approach the underlying sand layer. The medium-fine sand clearly injects and disrupts a thin gravel layer at the base of the silt-clay unit. The relationships are best seen where contrast is enhanced by the presence of darkening organic material in the gravel. Virtually identical structural associations have been recorded in sediments damaged by contemporary earthquakes. Figures 6 and 7 illustrate examples from the 30 April 1989 earthquake in Venezuela, as reported by Audemard & Santis (1991).

## Discussion and conclusions

The geometry of the fissures suggests brittle-type failure within the silt-clay layer. The patterns are similar to those produced experimentally by subjecting a cake of clay to tension (Cloos 1955). Antithetic and synthetic cracking can be expected, with en echelon arrays within the main fissure suite. Such patterns are characteristic of surface strains associated with flow-type failure at depth.

The presence of sand-free fissures and the general lack of evidence of forceful injection suggest that fine sand was emplaced in fissures after ground cracking. The sand would have been transported by water, sometimes as far as the surface to produce ridges and mounds. Dewatering accounts for the eye witness report of surface water.

The excess pressure required to raise water through the thickness of the confining layer to a height of over 2 m above the piezometric surface may have

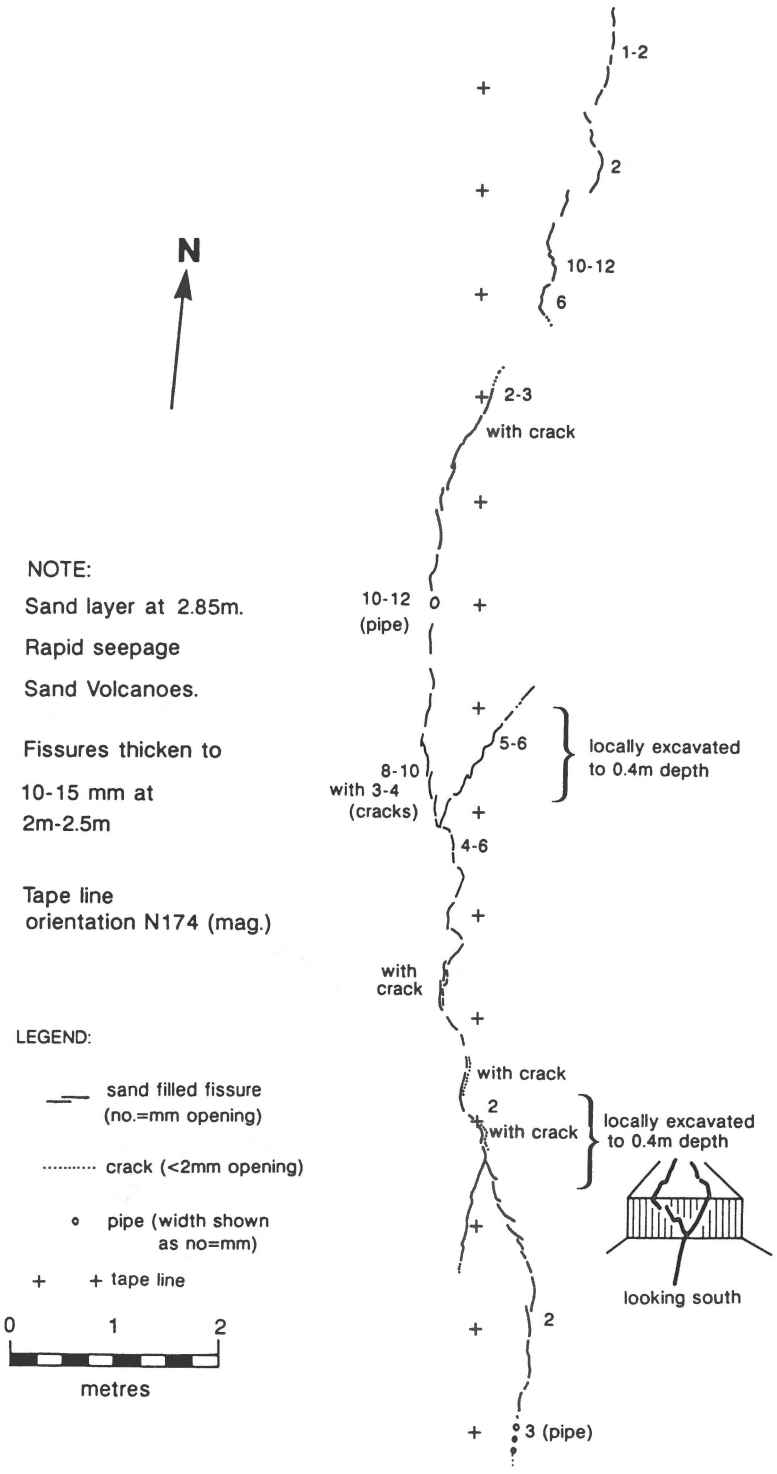


*Fig. 4.* Example map of fissure traces in Pit 3 at Herkenbosch

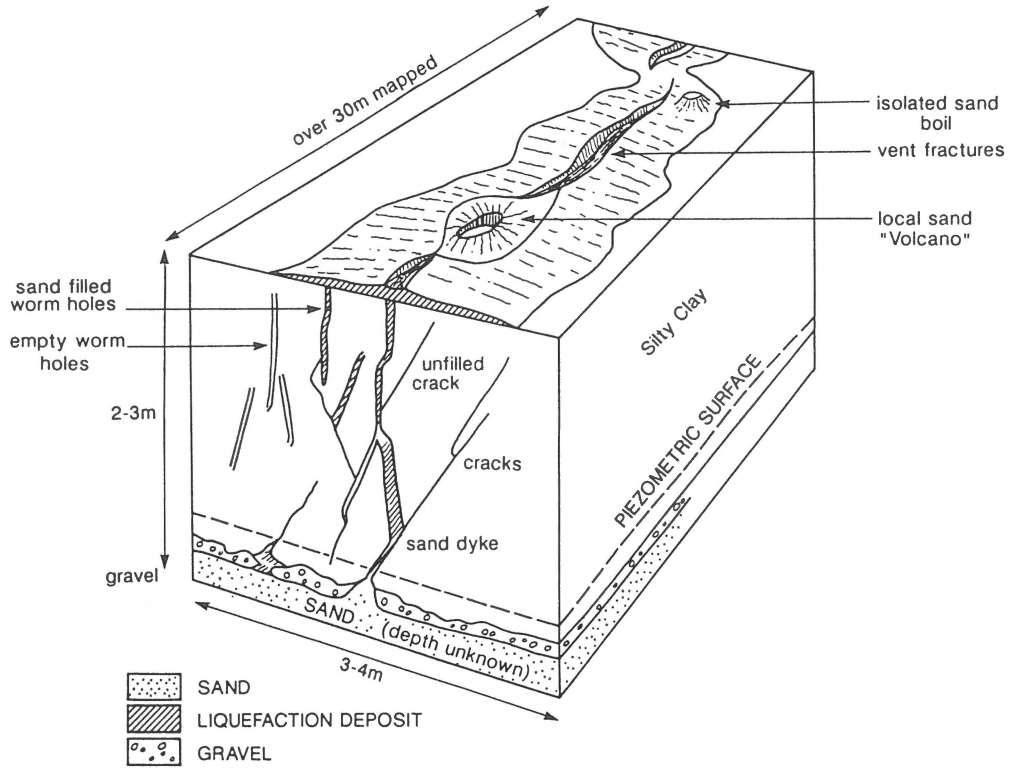


*Fig. 5.* Composite block diagram of liquefaction structures at Herkenbosch, April 1992.

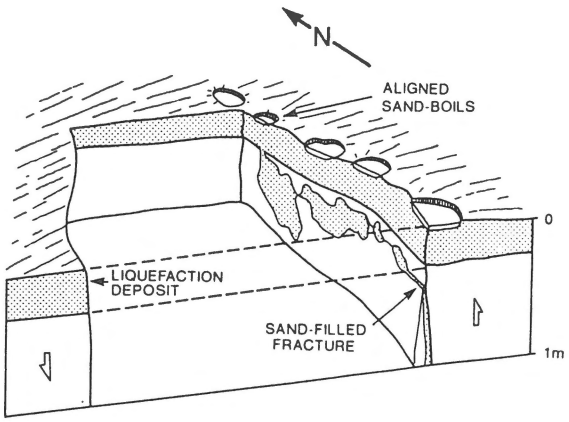


*Fig. 6.* Block diagram of Pit No. 9, Boca de Tocuyo, northwestern Venezuela, showing how the sand-filled fracture in cross-section matches perfectly with cone-mouth alignment (from Audemard & Santis 1991).

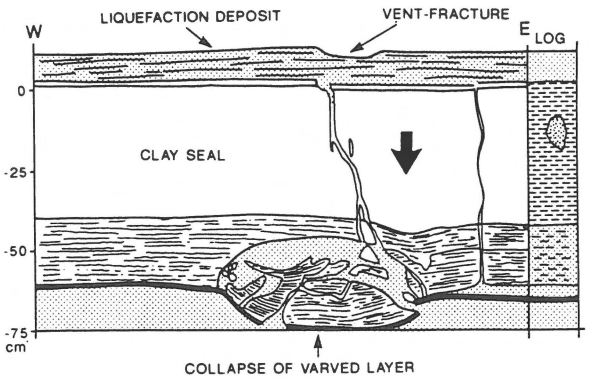


*Fig. 7.* North wall of Pit 12, Boca de Tocuyo, northwestern Venezuela, showing how void generation, produced by the extrusion of liquefied sands, induced the collapse of the bottom of the varved layer (from Audemard & Santis 1991).

been produced directly by dynamic loading and volume changes during liquefaction. However, an alternative explanation may be that such excess pressure may be a secondary result of the (slight?) horizontal displacements accompanying lateral spreading of flood plain deposits. Further investigations over a greater

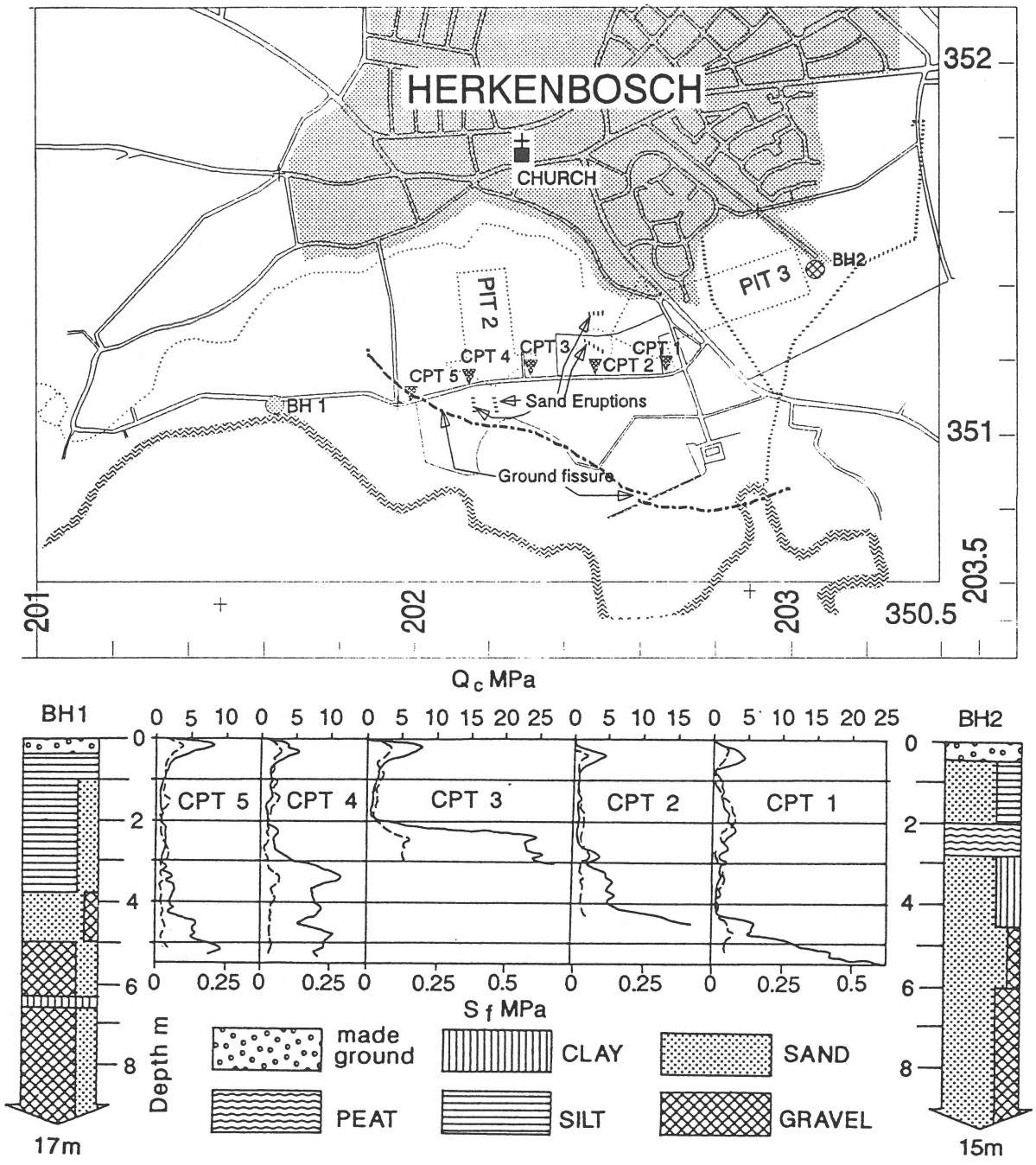


*Fig. 8.* Location plan and depth profiles of cone penetration test logs (CPT1 to CPT5) of cone-bearing resistance ($Q_c$) and sleeve friction ($S_f$) in MPa (dashed line) and borehole (BH1 and BH2) soil particle constituent profiles.

area will be required to establish widespread lateral spreading.

Another requirement of future investigations will be to excavate deeply (several meters) into the liquefied sand deposit. Only then will evidence for deep-layer liquefaction be found, perhaps in the form of soft-sediment deformation structures (seismites) with associated dewatering structures and fluidised injections (Davenport & Ringrose 1987, Davenport 1994).

The soil profile at Herkenbosch has been investigated subsequently by cone penetration tests (CPTs; Fig. 8. These show sands extending from between 2–4 m and maximum penetration depths varying from 3–5 m. Penetration probably stops as the gravel content in the sands increases. Existing boreholes on either side of the CPT traverse line indicate sands and gravels below 4 m depth, showing variation in the gravel-sand fraction.

## Acknowledgements

We thank our colleagues and students for support in discussion and field work, particularly those who helped with excavation and sampling. Special thanks go to members of the Seismological Unit of Royal Netherlands Meteorological Institute, Soil Mechanics (Delft) and the Geological Survey of the Netherlands (RGD) who provided data and guidance to J.M.J.L. during his thesis study.

## References

Ahorner, L. 1993 Erfahrungen aus dem Erdbeben bei Roermond am 13. April 1992. Separatdruck aus: Schweizerische Pool für Erdbeben-versicherung 14 – Geschäftsbericht, Bern: 10–26

Audemard, F.A. & F. de Santis 1991 Survey of liquefaction structures induced by recent moderate earthquakes – Bull. Int. Assn. Eng. Geol. 44: 5–16

Cloos, E. 1955 Experimental analysis of fracture patterns – Bull. Geol. Soc. Am. 66: 241–256

Davenport, C.A. 1994 Geotechnical consequences of ground motion: Hazard perspectives – Geol. Mijnbouw, this issue

Davenport, C.A. & P.S. Ringrose 1987 Deformation of Scottish Quaternary sediment sequences by strong earthquake motions. In: M.E. Jones & R.M.F. Preston (eds.): Deformation of Sediments and Sedimentary Rocks – Geol. Soc. Lond. Spec. Publ. 29: 299–314

Dienst Grondwater Verkenning TNO 1974 Grondwaterkaart van Nederland – Venlo, 52 O (1 : 50,000) en Centrale Slenk (Oost Brabant) (1 : 100,000)

Donovan, N.C. 1973 A statistical evaluation of strong motion data including the February 9, 1971 San Fernando earthquake – Proc. 5th World Conf. Earthq. Eng. Rome, 1: 1252–1261

Evernden, J.F. & J.M. Thomson 1985 Predicting seismic intensities. In: J.I. Ziony (ed.): Evaluating earthquake hazards in the Los Angeles region – An earth science perspective – US Geol. Surv. Prof. Paper 1360: 151–202

Joyner, W.B. & T.E. Fumal 1985 Predictive mapping of earthquake ground motion. In: J.I. Ziony (ed.): Evaluating earthquake hazards in the Los Angeles region – An earth science perspective – US Geol. Surv. Prof. Paper 1360: 203–220

Lap, J.M.J. 1987 Earthquake-induced liquefaction potential in the area south of Eindhoven, the Netherlands – Mem. Centre Eng. Geol. Netherlands 47: 40 pp

Maurenbrecher, P.M., D.G. Price & W. Verwaal 1994 Technical note on the 1992 Brunssummerheide landslide in Limburg, the Netherlands – Geol. Mijnbouw, this issue

Nason, R. 1982 Seismic intensity studies in the Imperial Valley. In: The Imperial Valley Earthquake of October 15, 1979 – US Geol. Surv. Prof. Paper 1254: 259–264

Seed, H.B. & I.M. Idriss 1971 Simplified procedure for evaluating soil liquefaction potential – Am. Soc. Civil Eng., J. Soil Mech. Found. Div 97 (9): 1249–1273

Tinsley, J.C., T.L. Youd, D.M. Perkins & A.T.F. Chen 1985 Evaluating liquefaction potential. In: J.I. Ziony (ed.): Evaluating earthquake hazards in the Los Angeles region – An earth science perspective – US Geol. Surv. Prof. Paper 1360: 263–316

Trifunac, M.D. & A.G. Brady 1975 On the correlation of seismic intensity with peaks of recorded strong ground motion – Bull. Seismol. Soc. Am. 65: 139–162